18. I. K. Dev, B. B. Yates, J. Leong, W. S. Dallas, *Proc. Natl. Acad. Sci. U.S.A.* **85**, 1472 (1988).
19. The 64 alleles of *thyA* with different codons at position 146 of the coding sequence were constructed as follows. First, a unique Nhe I site was introduced through a $Gly^{429} \rightarrow Ala$ substitution in the *thyA* coding region by site-directed mutagenesis (*26*) of plasmid pTSO (*16*) to yield plasmid pTSO1. Oligonucleotides THY1 (5′-CTGGATAAAATGGCGCTAGCACCGTGCCATGCATTC-3′) and THY2 (5′-TCTGCCACATAGAACTGGAAGAATGCATGGCACGGT-3′) were used for this mutation, which preserved the sense of the codon thus mutated. Plasmid pTSO1 was then digested with Nhe I and Nsi I to remove from the *thyA* coding region an 18–base pair fragment containing codon 146 (UGC). All 64 oligonucleotides of the *thyA* coding sequence from nucleotides 427 to 444 and the 64 oligonucleotides of the partial reverse sequence were constructed (GENAXIS Biotechnology, Montigny le Bretonneux, France). The 64 pairs of complementary oligonucleotides were annealed and ligated with the digested plasmid pTSO1.
20. Cysteine gradient plates were generated as described in the legend to Fig. 1B. The effects of L-valine alone could not be directly examined because exogenous L-valine is known to inhibit growth of *E. coli* K12 in minimal medium (*27*). This inhibition is relieved if L-isoleucine is also supplied. Thus, the Ile-Val dipeptide was used as a valine source, because this dipeptide is transported across the cell membrane and then broken down to isoleucine and valine (*28*).
21. Supplementary material is available on *Science* Online at www.sciencemag.org/cgi/content/full/292/5516/501/DC1.
22. M. J. Pine, *Antimicrobiol. Agents Chemother.* **13**, 676 (1978).
23. *Escherichia coli* chromosomal DNA was extracted using a DNeasy Tissue Kit (Qiagen GmbH, Hilden, Germany) following the instructions of the manufacturer. PCR to amplify the *valS* gene was performed as follows: denaturation at 94°C for 3 min, followed by 30 cycles of 30 s at 94°C, annealing at 57°C for 30 s, and primer extension at 72°C for 200 s. The final step was a primer extension at 72°C for 600 s. The reaction was carried out using 2 units of Vent DNA polymerase (New England Biolabs, Beverly, MA) and 100 ng of chromosomal DNA in a 100-μl reaction mixture. The following primers were used: VAL1 (5′-GGGGAATTCGGTGTGTGAAATTGCCGCAGAACG-3′), and VAL2 (5′-GGCAAGCTTTCAGGTATTTGCTGCCCAGATCGA-3′). Two independent PCR amplification products of each mutant were sequenced (GENAXIS Biotechnology).
24. L. Lin, S. P. Hale, P. Schimmel, *Nature* **384**, 33 (1996).
25. O. Nureki *et al.*, *Science* **280**, 578 (1998).
26. M. Ansaldi, M. Lepelletier, V. Mejean, *Anal. Biochem.* **234**, 110 (1996).
27. M. De Felice *et al.*, *J. Mol. Biol.* **156**, 1 (1977).
28. A. J. Sussman C. Gilvarg, *Annu. Rev. Biochem.* **40**, 397 (1971).
29. C. Richaud *et al.*, *J. Biol. Chem.* **268**, 26827 (1993).
30. E. Schmidt, P. Schimmel, *Biochemistry* **34**, 11204 (1995).
31. L. Lin, P. Schimmel, *Biochemistry* **35**, 5596 (1996).
32. L. M. Guzman, D. Belin, M. J. Carson, J. Beckwith, *J. Bacteriol.* **177**, 4121 (1995).
33. T. L. Hendrickson, T. K. Nomanbhoy, P. Schimmel, *Biochemistry* **39**, 8180 (2000).
34. K. Gevaert, J. Vandekerckhove, *Electrophoresis* **21**, 1145 (2000).
35. We thank A. Ullmann, M. Goldberg, M. Schwartz, and G. Cohen for encouraging initial efforts in the Pasteur Institute and M. A. Marahiel for his support. We thank J. Weissenbach for partial support in the Genoscope and P. Brooks for advice in writing the manuscript. We thank the TSRI mass spectrometry facility and J. Wu for performing the analysis, M. Lovato for the clone of AlaXp, T. Nomanbhoy for his constant help, and M. Berlyn from the *E. coli* Genetic Stock Center for a gift of strains. This work was supported by grant GM23562 from the National Institutes of Health and by a fellowship from the National Foundation for Cancer Research. H.D.M. was a Ph.D. fellow of the Stiftung Stipendien-Fonds des Verbandes der Chemischen Industrie. T.L.H. was an NIH postdoctoral fellow.

27 November 2000; accepted 14 February 2001

Cooperation and Competition in the Evolution of ATP-Producing Pathways

Thomas Pfeiffer,[1]* Stefan Schuster,[2] Sebastian Bonhoeffer[1]*†

Heterotrophic organisms generally face a trade-off between rate and yield of adenosine triphosphate (ATP) production. This trade-off may result in an evolutionary dilemma, because cells with a higher rate but lower yield of ATP production may gain a selective advantage when competing for shared energy resources. Using an analysis of model simulations and biochemical observations, we show that ATP production with a low rate and high yield can be viewed as a form of cooperative resource use and may evolve in spatially structured environments. Furthermore, we argue that the high ATP yield of respiration may have facilitated the evolutionary transition from unicellular to undifferentiated multicellular organisms.

Heterotrophic organisms obtain their energy by the degradation of organic substrates into products with lower free energy. The free energy difference between substrate and product can in part be conserved by production of ATP and in part be used to drive the degradation reaction. The maximal ATP yield is obtained if the entire free energy difference is conserved as ATP. However, in this case the reaction is in thermodynamic equilibrium, and therefore the rates of substrate degradation and ATP production vanish. If some of the free energy difference is used to drive the reaction, the rate of ATP production increases with decreasing yield until a maximum is reached. Hence, for fundamental thermodynamic reasons there is always a trade-off between yield (moles of ATP per mole of substrate) and rate (moles of ATP per unit of time) of ATP production in heterotrophic organisms (*1*–*4*).

A trade-off between yield and rate of ATP production is also present in sugar degradation by fermentation and respiration. In the presence of oxygen and sugars, many organisms are in principle capable of using both pathways to produce ATP. Because the ATP production rate of respiration is rapidly saturated at high levels of resource or limited oxygen supply (*5*–*8*), these organisms can choose, at least in the evolutionary sense, to increase the rate of ATP production by using fermentation in addition to respiration. However, because the yield of fermentation is much lower than that of respiration (2 mol versus about 32 mol of ATP per mole of glucose), the use of fermentation in addition to respiration increases the rate of ATP production at the cost of a lower total yield.

If energetic limitation is an important factor for organisms in their natural environment, we then expect that the properties of ATP-producing pathways have been under strong selection pressure during evolution. The existence of a trade-off between yield and rate of ATP production leads to the following question: Under what conditions is it favorable to use a pathway with high yield but low rate, as opposed to a pathway with low yield but high rate? A cell using a pathway with high yield and low rate can produce more ATP (and thus more offspring) from a given amount of resource. However, this advantage disappears when the cell is in resource competition with cells that produce ATP at a higher rate but a lower yield. While only those cells that consume the resource more rapidly benefit from the higher rate of ATP production, all competitors exploiting the resource share the consequences of the more rapid resource exhaustion (*9*).

The competition between cells with different properties in ATP production can be illustrated with a simple population biological model. Assume that a resource S is produced at a constant rate v and is consumed by n different strains of cells, N_i, at a rate of $J_i^S(S)$ per cell. We assume that the growth rates of the strains are energetically limited and proportional to the rate of ATP produc-

[1]Friedrich Miescher Institute, Post Office Box 2543, CH-4002 Basel, Switzerland. [2]Max Delbrück Center for Molecular Medicine, D-13092 Berlin, Germany.

*Present address: Experimental Ecology and Theoretical Biology, Eidgenössische Technische Hochschule (ETH) Zürich, CH-8092 Zürich, Switzerland.
†To whom correspondence should be addressed. E-mail: bonhoeffer@eco.umnw.ethz.ch

tion, $cJ_i^{ATP}(S)$, where c is a proportionality constant (*10, 11*). Finally, we assume that the death rate d of all strains is the same. Thus, the population dynamics are given by

$$dS/dt = v - \sum_{i=1}^{n} N_i J_i^S(S)$$

$$dN_i/dt = cJ_i^{ATP}(S)N_i - dN_i$$

$$(i = 1, \ldots, n) \qquad (1)$$

If there is only one strain ($n = 1$), then the steady-state level of the population is given by $N_1 = y_1 vc/d$, where the yield of ATP production, $y_1 = J_1^{ATP}/J_1^S$, is given by the ratio of the rates of ATP production and resource consumption. Hence, the population size N_1 depends on the yield but not the rate of ATP production (*12*). If several strains ($n > 1$) compete for the resource, the outcome of competition is determined by the highest growth rate, and hence by the highest rate of ATP production. This implies that a cell population using a pathway with low yield but high rate can invade and replace a cell population using a pathway with high yield and low rate (*4*). However, the invading cells eventually establish a smaller population because of the lower ATP yield. The resulting evolutionary dilemma is analogous to the "tragedy of the commons," a framework widely used in evolutionary game theory to describe evolution toward the inefficient use of a common resource (*13*). In energy metabolism, evolution may work to select the less efficient pathway if cells are in competition for a shared resource.

The evolutionary dilemma arises only if there is competition for shared resources. Thus, according to our hypothesis, pathways with high rate but low yield of ATP production (such as fermentation) should primarily be observed in association with the exploitation of external resources. Indeed, microorganisms growing on external sugar resources, such as *Saccharomyces*, *Mucor*, and *Lactobacilli*, which are present in the early phases of decomposition of organic material, use fermentation for ATP production even in the presence of oxygen (*7, 14, 15*). In contrast, organisms metabolizing internal resources such as ingested food items are expected to use pathways with high yield but low rate of ATP production. In line with our hypothesis, higher animals indeed mostly use respiration to produce ATP from ingested sugar resources. Fermentation is observed only in situations where very high rates of ATP production are essential, as for example in muscle cells.

Further interesting differences in ATP production between microorganisms and higher organisms are manifest in the specific design of oxidative phosphorylation. The P/O stoichiometry (moles of ATP produced during the oxidation of NADH, the reduced form of nicotinamide adenine dinucleotide) in mammalian mitochondria (rat liver) is 2.5 or higher (*16–18*). It has been reported that this value does not maximize the rate of ATP production, but rather trades a lower rate against a higher yield, as is expected for higher organisms metabolizing internal resources (*1, 3*). In yeasts, such as *S. cerevisiae* and *Candida utilis*, lower stoichiometries have been reported [1.5 and 2.0, respectively (*7, 19*)], suggesting that in these organisms the stoichiometries of oxidative phosphorylation are adjusted to produce ATP at a higher rate. Moreover, it has been reported that fermentation is designed to maximize the rate of ATP production (*2, 20*). This is in agreement with our hypothesis, because fermentation should be used in addition to respiration only when high rates rather than high yields of ATP production are required. Finally, further evidence suggestive of the relevance of tradeoffs between rate and yield in natural systems stems from the observation that certain organisms, such as *Escherichia coli* and *S. cerevisiae*, appear to be capable of regulating the stoichiometry of oxidative phosphorylation, and thus ATP yield and rate, physiologically (*21, 22*). This could enable these organisms to adjust rate and yield of ATP production to varying environmental conditions.

One way to benefit from the high ATP yield of respiration is to avoid competition by cooperating with the other consumers of a shared resource. The exclusive use of respiration in the cells of a multicellular organism can be interpreted as such cooperation. In

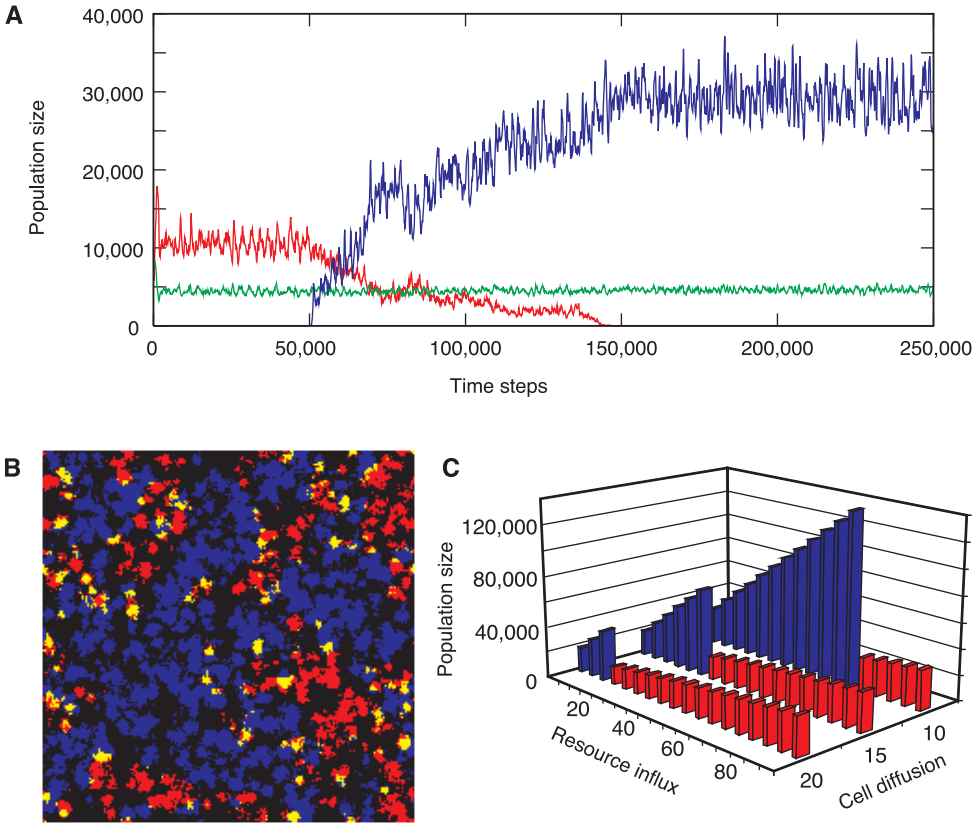

Fig. 1. Competition between respirators (blue) and fermenters (red) in a spatially structured environment. (**A**) A typical simulation of the spatial model (Eq. 2). The green line represents the resource level. In the first 50,000 time steps, only fermenters are present. Respirators are then introduced into the system at low frequency. In this simulation, respirators eventually outcompete fermenters. Parameters: cell diffusion $D^N = 20$, resource influx $R = 15$. See (*4, 27*) for further details. (**B**) A snapshot of the spatial distribution of fermenters and respirators during a typical simulation. Sites where both fermenters and respirators are present are depicted in yellow. Empty sites are black. Parameters: $D^N = 20$, $R = 15$. (**C**) The outcome of competition as a function of resource influx and cell diffusion rate. High rates of resource influx R and cell diffusion D^N favor fermenters. Despite increasing resource influx, the population size decreases when fermenters outcompete respirators.

contrast to most other cells in a multicellular organism, tumor cells often use fermentation (*23, 24*). Thereby they may gain a selective advantage when in competition for energy resources with other cells of the organism. Thus, tumor cells can be viewed as leaving the realm of cooperation in a multicellular organism.

Depending on the ecological properties of the habitat, cooperative resource use could also evolve in populations of unicellular organisms. The evolution of cooperation is generally facilitated in spatially structured environments (*25, 26*). To illustrate the effect of spatial structure on the evolution of cooperative resource use, we extend the above model to a spatial model including diffusion of cells (at a rate D^N) and of resource (at a rate D^S),

$$\partial S/\partial t = v - \sum_{i=1}^{n} N_i J_i^S(S) - D^S \nabla^2 S$$

$$\partial N_i/\partial t = cJ_i^{\mathrm{ATP}}(S)\,N_i - dN_i - D^N \nabla^2 N_i \qquad (i = 1, \ldots, n), \qquad (2)$$

where ∇^2 is the Laplace operator. In Fig. 1 we show a simulation of spatial resource competition between an exclusively respiring strain (respirator) and a strain that uses fermentation in addition to respiration (fermenter). The simulations are based on the following assumptions: (i) The rate of resource influx v is stochastic in space and time. (ii) The rates of resource consumption $J_i^S(S)$ are saturating functions of the resource S. (iii) At high levels of resource, the fermenters have a considerably higher rate of resource consumption. (iv) Both fermenters and respirators have the same rate of ATP production by respiration, but the fermenter additionally produces ATP by fermentation. To account for discrete strain population size, we assigned integer values to N_i. [For details of the simulation, see (*4, 27*).]

The simulations shown in Fig. 1 illustrate two points. First, as the rate of resource influx v increases, fermenters progressively outperform respirators. This is because higher resource influx rates lead to increased competition, essentially because the population density increases, which in turn makes it more likely that respirators suffer from local competition with fermenters. Second, at higher cell diffusion rates, fermenters perform better than respirators. This is because any metabolic type, whether a respirator or a fermenter, performs worse when in competition with surrounding fermenting cells, which rapidly exhaust the resource locally. At low cell diffusion rates, cells tend to be surrounded by their own metabolic type. As a consequence, fermenters perform worse. Thus, the spatial structure resulting from low diffusion rates (of cells and resource) gives fermenters a disproportionately higher selective disadvantage. As the diffusion rates of cells or resource increase, cells increasingly compete globally for the same resource, and in the limiting case, fermenters outcompete respirators as in the nonspatial model (Eq. 1).

The correlation between the exclusive use of respiration and spatial aggregation, which appears in our simulations, can be observed in dimorphic fungi. These microorganisms occur in two different phenotypes: a mycelial, multicellular form and a yeast-like, unicellular form. Interestingly, these phenotypes differ in their sugar metabolism. *Mucor racemosus*, for example, uses fermentation in the unicellular stage but respiration in the multicellular stage (*14*). In other *Mucor* species it was shown that fermentation is strictly associated with the yeast-like form, because inhibition or knockout of the respiration pathway results in the suppression of the mycelial form (*28, 29*). Furthermore, in agreement with the spatial model, fermentation is used at high glucose concentrations, whereas the respiring phenotype is observed at low glucose concentrations.

Presumably the best studied facultatively multicellular organisms are *Myxococcus* and *Dictyostelium*. Both feed almost exclusively on nonfermentable resources. Therefore, a trade-off between yield and rate resulting from the use of fermentation and respiration does not appear to exist in their natural habitat. However, it is possible that the trade-off is manifest in the specific design of the respiratory pathway. A testable prediction of our hypothesis would be that these organisms evolved a P/O stoichiometry that trades maximal rate against higher yield of ATP production in the multicellular stage.

The fact that the switch from fermentation to respiration in dimorphic fungi is tightly coupled to the transition from the yeast-like to the mycelial form suggests that the high ATP yield of respiration could have played a key role in the evolutionary transition of heterotrophic organisms from single cells to early, undifferentiated forms of multicellularity. In heterotrophic eukaryotes, aerobic respiration evolved after the rise of oxygen in the atmosphere by symbiosis with respiring bacteria, the ancestors of present-day mitochondria (*30*). Respiration not only allowed these organisms to produce ATP with higher yield, but also enabled them to use previously unexploitable, nonfermentable resources for ATP production. Multicellularity became abundant after the evolution of respiration and has probably evolved independently more than 10 times (*31–33*). The simulations of the spatial model suggest that after respiration had evolved, aggregating cells may have benefited from respiration (and, equivalently, respiring cells may have benefited from aggregation). Thus, the high ATP yield of respiration, which is a reward of cooperative resource consumption, might constitute an evolutionary advantage to respiring multicellular organisms (*34, 35*). Importantly, this advantage also accrues to undifferentiated multicellular organisms, whereas most other evolutionary advantages of multicellularity arise from cell differentiation and specialization, which presumably appeared after the evolution of undifferentiated multicellular organisms.

References and Notes

1. F. Angulo-Brown, M. Santillan, E. Calleja-Quevedo, *Nuovo Cim.* **17D**, 87 (1995).
2. T. G. Waddell, P. Repovic, E. Melendez-Hevia, R. Heinrich, F. Montero, *Biochem. Educ.* **27**, 12 (1999).
3. J. W. Stucki, *Eur. J. Biochem.* **109**, 269 (1980).
4. See supplementary material at *Science* Online (www.sciencemag.org/cgi/content/full/VOL/ISSUE/PAGE/DC1).
5. A. Fiechter, F. K. Gmunder, *Adv. Biochem. Eng. Biotechnol.* **39**, 1 (1989).
6. E. Postma, C. Verduyn, W. A. Scheffers, J. P. Van Dijken, *Appl. Environ. Microbiol.* **55**, 468 (1989).
7. J. P. van Dijken, R. A. Weusthuis, J. T. Pronk, *Antonie Van Leeuwenhoek* **63**, 343 (1993).
8. D. Voet, J. G. Voet, *Biochemistry* (Wiley, New York, ed. 2, 1995).
9. The evolutionary importance of trade-offs is discussed in the literature on life history theory [R. H. MacArthur, E. O. Wilson, *The Theory of Island Biogeography* (Princeton Univ. Press, Princeton, NJ, 1967); S. C. Stearns, *The Evolution of Life Histories* (Oxford Univ. Press, Oxford, 1992); D. A. Roff, *The Evolution of Life Histories* (Chapman & Hall, New York, 1992)]. Much of evolutionary biology is based on the assumption of trade-offs between properties that determine the life history of an organism. Although such trade-offs commonly are based on heuristic assumptions, in the case of ATP production the trade-off between rate and yield can be derived from biochemical and physical principles.
10. T. Bauchop, S. R. Elsden, *J. Gen. Microbiol.* **23**, 457 (1960).
11. O. M. Neijssel, M. J. Teixeira de Mattos, *Mol. Microbiol.* **13**, 172 (1994).
12. Provided the rates of ATP production as a function of the resource level do not intersect, it can be shown that only one strain, k, persists in equilibrium. This strain is characterized by $J_k^{\mathrm{ATP}}(S) > J_j^{\mathrm{ATP}}(S)$ for all $j \neq k$.
13. G. Hardin, *Science* **162**, 1243 (1968).
14. C. B. Inderlied, P. S. Sypherd, *J. Bacteriol.* **133**, 1282 (1978).
15. B. Poolman, *FEMS Microbiol. Rev.* **12**, 125 (1993).
16. P. C. Hinkle, M. A. Kumar, A. Resetar, D. L. Harris, *Biochemistry* **30**, 3576 (1991).
17. C. P. Lee, Q. Gu, Y. Xiong, R. A. Mitchell, L. Ernster, *FASEB J.* **10**, 345 (1996).
18. A. D. Beavis, A. L. Lehninger, *Eur. J. Biochem.* **158**, 315 (1986).
19. T. Onishi, K. Kawaguchi, B. Hagihara, *J. Biol. Chem.* **241**, 1797 (1966).
20. R. Heinrich, S. Schuster, *The Regulation of Cellular Systems* (Chapman & Hall, New York, 1996).
21. M. W. Calhoun, K. L. Oden, R. B. Gennis, M. J. de Mattos, O. M. Neijssel, *J. Bacteriol.* **175**, 3020 (1993).
22. V. Fitton, M. Rigoulet, R. Ouhabi, B. Guerin, *Biochemistry* **33**, 9692 (1994).
23. H. G. Crabtree, *Biochem. J.* **23**, 536 (1929).
24. O. Warburg, *Science* **123**, 309 (1956).
25. L. Chao, B. R. Levin, *Proc. Natl. Acad. Sci. U.S.A.* **78**, 6324 (1981).
26. M. A. Nowak, R. M. May, *Nature* **359**, 826 (1992).
27. The resource consumption rates used in the simulations are given by $J_1^S(S) = S/(1 + S)$ and $J_2^S(S) = 100S/(100 + S)$, where the indices 1 and 2 refer to

respirators and fermenters, respectively. Assuming a yield of 32 mol of ATP per mole of glucose, the ATP production of respiration is given by $J_1^{ATP}(S) = 32J_1^S(S)$. In fermentation the remainder of the resource uptake, $J_2^S(S) - J_1^S(S)$, is fermented with a yield of 2 ATP. Thus, the total ATP production of a fermenter is given by $J_2^{ATP}(S) = 32J_1^S(S) + 2[J_2^S(S) - J_1^S(S)]$. For computer simulations, the model (Eq. 2) was transformed into the corresponding difference equations [W. H. Press, S. A. Teukolsky, W. T. Vetterling, B. P. Flannery, *Numerical Recipes* (Cambridge Univ. Press, Cambridge, ed. 2, 1992)]. All simulations were performed on a 100 × 100 grid (except for the 200 × 200 grid in Fig. 1B) with a grid unit length of 1 and a time step of 0.001. In all simulations we chose $c = 1$, $d = 10$, and $D^S = 1$. An amount of resource, R, was added to a site stochastically with a probability of 0.0005 per time step. N_i was rounded up or down probabilistically (with p and $p - 1$, respectively, where p is the fractional part of N_i) to reflect discrete cell numbers. All simulations were started with fermenting cells only. Between time steps 50,000 and 100,000, respiring cells were added with probability 10^{-5} per site and time step. The population size shown in Fig. 1C was averaged over time steps 200,000 to 250,000.

28. P. J. Rogers, G. D. Clark-Walker, P. R. Stewart, *J. Bacteriol.* **119**, 282 (1974).
29. B. E. Schulz, G. Kraepelin, W. Hinkelmann, *J. Gen. Microbiol.* **82**, 1 (1974).
30. L. Margulis, *Symbiosis in Cell Evolution* (Freeman, San Francisco, 1981).
31. R. E. Dickerson, *Sci. Am.* **242**, 137 (March 1980).
32. J. T. Bonner, *Integrat. Biol.* **1**, 27 (1998).
33. J. Maynard Smith, E. Szathmáry, *The Major Transitions in Evolution* (Freeman, Oxford, 1995).
34. We argue that aggregation of cells and the formation of multicellular organisms allowed cells to benefit from the high ATP yield resulting from the exclusive use of respiration. This is in contrast to the hypothesis that after the evolution of respiration, the high ATP yield of respiration gave cells an "energetic luxury" that subsequently allowed them to increase genome size and evolve multicellularity [T. Vellai, K. Takács, G. Vida, *J. Mol. Evol.* **46**, 499 (1998)].
35. Our line of reasoning only applies to heterotrophic organisms, because it is based on competition for an exhaustible resource and a trade-off between rate and yield of ATP production. In phototrophic organisms there is no evolutionary dilemma, because light is an inexhaustible resource. As a consequence, phototrophic organisms need not overcome this evolutionary dilemma for the evolution of multicellularity.
36. We thank M. Ackermann, M. Brown, M. Flor, T. Killingback, D. Krakauer, and P. Schmid-Hempel for helpful discussions and critical review of the manuscript. Support from the Novartis Research Foundation (T.P. and S.B.) and the Deutsche Forschungsgemeinschaft (S.S.) is gratefully acknowledged.

7 December 2000; accepted 2 March 2001

astray, a Zebrafish *roundabout* Homolog Required for Retinal Axon Guidance

Cornelia Fricke,[1] Jeong-Soo Lee,[1] Silke Geiger-Rudolph,[2] Friedrich Bonhoeffer,[3] Chi-Bin Chien[1]*

As growing retinotectal axons navigate from the eye to the tectum, they sense guidance molecules distributed along the optic pathway. Mutations in the zebrafish *astray* gene severely disrupt retinal axon guidance, causing anterior-posterior pathfinding defects, excessive midline crossing, and defasciculation of the retinal projection. Eye transplantation experiments show that *astray* function is required in the eye. We identify *astray* as zebrafish *robo2*, a member of the Roundabout family of axon guidance receptors. Retinal ganglion cells express *robo2* as they extend axons. Thus, *robo2* is required for multiple axon guidance decisions during establishment of the vertebrate visual projection.

During development of the retinotectal projection, retinal ganglion cell (RGC) axons navigate through a series of environments. They first grow toward the optic disc, exit the eye at the ventral fissure, and grow along the base of the ventral diencephalon, where they meet the contralateral retinal axons, forming the optic chiasm. They then progress into the optic tract and project topographically to their central targets, primarily the optic tectum in nonmammalian vertebrates. There is a growing understanding of the molecular mechanisms that specify retinotectal topography (*1*–*3*) and that guide retinal axons within the eye (*4*, *5*), but to date few axon guidance molecules have been shown in vivo to function between eye and tectum (*6*, *7*).

We have used the zebrafish to identify such guidance molecules and study their functions in vivo. The transparency of the larvae in combination with the amenability of this model organism to genetics has made it possible to directly visualize the retinal projection and isolate genes required for RGC axon guidance (*8*). *astray* (*ast*) (*9*) is one of the key genes isolated in this large-scale screen. Four alleles (*ti272z*, *te378*, *tl231*, and *te284*) have been found, all with similar phenotypes. Compared to wild type (WT), in which the retinotectal projection at 5 days postfertilization (dpf) is exclusively contralateral, RGC axons in *ast/ast* embryos exhibited misprojections to ipsilateral tectum and several extratectal targets (*9*) (Fig. 1).

Confocal analysis after lipophilic dye labeling at 5 dpf (*10*) showed that after *ast* RGC axons exited the eye, they made a wide variety of pathfinding errors at multiple locations (Fig. 1), predominantly at or after the midline. Anterior-posterior guidance defects were common, including anterior projections into diencephalon and telencephalon, and posterior projections to both ipsilateral and contralateral ventral hindbrain (VHB) (Fig. 1, C to F). Anteriorly projecting axons often reached as far as presumptive olfactory bulb; they also often recrossed the midline, then continued anteriorly or turned posteriorly (Fig. 1E). Axons recrossed the midline in at least three distinct locations: VHB, ventral telencephalon near the anterior commissure (AC), and dorsally in the posterior commissure (PC); the latter was a common route by which retinal axons reached the ipsilateral tectum (Fig. 1C). In strong phenotypes, the optic tract showed severe defasciculation (Fig. 1, E and F). Occasionally, the optic chiasm formed abnormally: The optic nerve was unusually distant from the contralateral optic nerve, or split into two or more parts at the midline (Fig. 1I). Retinal axons also sometimes projected into the opposite eye. Axons from all four retinal quadrants showed pathfinding errors; however, axons that reached the tectum appeared to project topographically (*9*, *11*). Thus, *ast* function is required for midline crossing as well as several other axon guidance decisions.

All four *ast* alleles are recessive and cause a similar array of phenotypes, suggesting that they are loss-of-function mutations. Phenotypic strength varied widely between embryos, even within clutches, and the two eyes sometimes showed different phenotypes. Even in the embryos with the strongest phenotypes, a subset of axons reached the contralateral tectum. Scoring *ast*/+ × *ast*/+ incrosses (*10*) showed three completely penetrant alleles [*ti272z* (24.5% mutant, $n = 335$ embryos), *te378* (25.8%, $n = 159$), and *tl231* (25.3%, $n = 182$)] and one weaker allele [*te284* (18.0%, $n = 133$)]. Supporting the conclusion that *te284* is weaker was the observation that often only a single eye of *te284* homozygotes showed a detectable phenotype, whereas in all *ti272z* homozygotes examined, both eyes showed mutant phenotypes. Projections to VHB (86%) and across the PC (78%) were more common than anterior projections (64%) (*ti272z* homozygotes, $n = 175$ eyes).

[1]Department of Neurobiology and Anatomy, University of Utah Medical Center, 50 North Medical Drive, Salt Lake City, UT 84132, USA. Abteilung [2]Genetik and [3]Physikalische Biologie, Max-Planck Institut für Entwicklungsbiologie, Spemannstrasse 35, D-72076 Tübingen, Germany.

*To whom correspondence should be addressed at Department of Neurobiology and Anatomy, 401 MREB, University of Utah Medical Center, 50 North Medical Drive, Salt Lake City, UT 84132, USA. E-mail: chi-bin.chien@hsc.utah.edu